

## Stability of Wakes behind Elongated Bluff Bodies at Incidence

A. Rao<sup>1</sup>, M. C. Thompson<sup>1</sup> and K. Hourigan<sup>1</sup>

<sup>1</sup>Fluids Laboratory for Aeronautical and Industrial Research (FLAIR),  
Department of Mechanical and Aerospace Engineering, 17 College Walk,  
Monash University, Clayton, Victoria 3800, Australia

### Abstract

Flow past elongated bluff bodies for Reynolds numbers  $Re \leq 500$  is investigated here for incident angles  $I \leq 20^\circ$ . Two-dimensional simulations are performed using a spectral element solver for elliptical shaped cylinders for aspect ratios  $AR \leq 2.5$  to first obtain the base flows, following which linear stability analysis is performed on the unsteady base flows to investigate the onset of three-dimensional modes. For low aspect ratio cylinders, the transition sequence from steady two-dimensional flow to unsteady three-dimensional flow (steady  $\rightarrow$  unsteady  $\rightarrow$  mode A  $\rightarrow$  mode B  $\rightarrow$  mode QP) closely resembles that of a circular cylinder for all incident angles. As the aspect ratio is increased, the onset of these transitions is delayed to higher Reynolds numbers for a given incidence angle, while the onset of the three-dimensional modes occurs at lower Reynolds numbers on increasing the incidence angles. The behaviour of the various three-dimensional modes is investigated in this parameter space.

### Introduction

Flow past bluff bodies has been investigated for over a hundred years and in recent decades, the two- and three-dimensional transitions past canonical bluff bodies have received more attention since the seminal works of [29, 30, 31]. Of particular interest is the route to turbulence through the various transitions as Reynolds number ( $Re = UD/\nu$ , where  $U$  is the flow velocity,  $D$  is the minor axis and  $\nu$  is the kinematic viscosity of the fluid) is increased [12]. For a circular cylinder, the onset of unsteady flow occurs at  $Re \simeq 47$  with the formation of Bénard-von Kármán vortex street that becomes three-dimensional around  $Re \simeq 190$  with the onset of a long wavelength instability that spans approximately four cylinder diameters, known as *mode A* instability. As the Reynolds number is increased, mode A gives way to a smaller wavelength instability known as *mode B* at  $Re \simeq 260$ , which spans approximately one cylinder diameter [31]. Numerical computations via linear stability analysis [1] and three-dimensional direct numerical simulations (DNS) by [27] confirmed the presence of these instabilities. Modes A and B were found to be synchronous modes with the underlying two-dimensional base flows and do not introduce any new frequency in the spanwise direction. Modes which are non-synchronous with the base flow have been observed in bluff body flows such as square shaped cylinders and are known as quasi-periodic modes or *mode QP* [2, 8]. Such modes usually occur at Reynolds numbers beyond the onset of modes A and B, as in the case of a circular cylinder at  $Re \simeq 380$  [3]. Subharmonic modes have also been observed in bluff bodies when the wake symmetry is broken, leading to a period doubling of the mode. Such modes have been observed in the wake behind

rings [24, 25], rotating cylinders [13, 14, 15, 16], square cylinders at an incident angle [22, 23] and when trip wires are placed in the proximity of bluff bodies [17, 32, 33]. Mode QP and mode C typically have spanwise wavelengths in between that of modes A and B. When these modes are resolved numerically via Floquet analysis, modes A and B lie on the positive real axis of a complex plane, while mode C lies on the negative real axis. Mode QP occurs in conjugate pairs and have real ( $\mu_{real}$ ) and imaginary components ( $\mu_{imag}$ ) of the Floquet multiplier.

Flow past elongated bluff bodies has garnered interest in the last few years with several researchers performing numerical and experimental simulations [4, 6, 9, 10, 11]. The wake of elliptical leading edge bluff bodies of aspect ratio  $AR = 2.5$ , (where  $AR = a/D$  is the aspect ratio, defined as the ratio of the major axis of the ellipse,  $a$ , to its minor axis,  $D$ ) was investigated by [20] and they observed a new three-dimensional mode, mode B', which was a synchronous mode with a spanwise wavelength of  $\simeq 2.4D$  and spatio-temporal characteristics similar to the mode B instability. This mode was also observed by [21] in their investigation of an elliptical cylinder of  $AR = 2$  for incidence angles  $I \leq 30^\circ$  at  $Re = 283.1$  and was labelled mode B\*. They performed linear stability investigations at this Reynolds numbers for various incidence angles, and reported a long wavelength mode of spanwise wavelength  $\lambda/D \geq 6$  at  $I = 15^\circ$  unstable to perturbations at higher incidence angles, which was observed alongside smaller wavelength modes. They also observed that the critical Reynolds number of onset for mode A instability was delayed to  $Re \simeq 330$  as compared to a circular cylinder. More recently, [7] performed linear stability analysis for elliptical cylinders  $AR \leq 2.4, Re \leq 500$  at  $I = 0^\circ$  and observed mode B' (labelled mode  $\hat{B}$  in their paper) for  $AR \geq 1.8$  and a long wavelength mode, mode  $\hat{A}$ , for  $AR \geq 1.2$  which had spatio-temporal characteristics similar to the mode A instability. Mode  $\hat{A}$  was previously observed in the wake of a rotating cylinder as mode G [14, 16], where the spanwise vortex structure of mode A and mode  $\hat{A}$  differed only in the downstream vortices. They observed that the transition sequence for the onset of three-dimensional modes no longer resembled that of a circular cylinder for  $AR \gtrsim 1.75$ .

This study builds upon the studies of [7] and [21], where numerical investigations are undertaken for elliptical cylinders for  $AR \leq 2.5, Re \leq 500$  and  $I \leq 20^\circ$ . Results from the linear stability analysis are presented as parameter maps depicting regions where three-dimensional modes are unstable to perturbations. The naming convention of the modes are retained from [7]. The numerical methodology is briefly described in the following section followed by the results from the numerical computations and conclusions.

## Numerical formulation and setup

The Navier-Stokes equations are solved using a spectral element formulation. The computational domain consists of quadrilateral elements that are concentrated around the elliptical cylinder to accurately capture the velocity gradients. These quadrilateral elements are further subdivided into internal node points, which are distributed according to Gauss-Legendre-Lobatto quadrature points. The velocity and pressure fields are represented by tensor products of Lagrangian polynomial interpolants. Spectral convergence is achieved as the polynomial order is increased [5]. The number of node points within each element ( $N \times N$ ) can be specified at runtime with the interpolating polynomial order in each direction being  $N - 1$ . A second-order fractional time-stepping technique is used to sequentially integrate the advection, pressure and diffusion terms of the Navier-Stokes equations forward in time. More details of the time-stepping scheme can be found in [26].

To investigate the stability of the flow to three-dimensional perturbations, stability analysis is carried out in the  $Re - I$  parameter space for various aspect ratios. The Navier-Stokes equations are linearised and the spanwise wavelengths are constructed as a set of Fourier modes. These equations are integrated forward in time and the growth of these perturbations is monitored. After several time periods, the fastest growing modes dominate the system. The Floquet multiplier ( $\mu$ ) is then computed; for  $\mu < 1$ , the perturbations decay and for  $\mu > 1$ , the perturbations grow and the flow transitions to three-dimensionality. Neutral stability is achieved when  $\mu = 1$ . More details on this method has can be found in [7, 17, 19, 18, 20, 24, 28].

The elliptical cylinder was located in the centre of the domain, with the inlet and lateral boundaries of domain being located  $60D$ , while the outlet boundary was located  $100D$  from the cylinder so that effects due to blockage were minimised. Spatial resolution studies were undertaken for  $AR = 1.1, 2$  and  $2.5$  at  $I = 0^\circ, 10^\circ$  and  $20^\circ$  at  $Re = 500$  by varying the number of internal node elements from  $N = 4$  to  $N = 11$ . For  $N = 8$ , the force coefficients and the shedding frequencies for the cases were well within 1% of those for the maximum polynomial order. Additionally, a time-step resolution study undertaken showed that the variation in the force coefficients and shedding frequencies were well within 1% of those for the maximum time-step used ( $\Delta t = 0.001$ ). Furthermore, the critical Reynolds number ( $Re_c$ ) for the onset of the three-dimensional modes at  $I = 0^\circ$  were in good agreement with that observed by [7].

## Results

Linear stability analysis was performed on the two-dimensional base flows obtained by time-marching the solutions for at least 400 non-dimensional time units. For the circular cylinder ( $AR = 1$ ), the onset of modes A, B and QP occurs at  $Re \simeq 190, 260$  and  $380$ , respectively [1, 3]. For  $AR = 1.1$ , the critical Reynolds number ( $Re_c$ ) for the onset of modes A and B decreases marginally ( $\Delta Re \simeq 4$ ) while that of mode QP increases marginally ( $\Delta Re \simeq 2$ ) as the incident angle is increased. Furthermore, the variation of the spanwise wavelength of these modes at onset does not vary with the incident angle.

At  $I = 0^\circ$ , [7] reported the onset of mode  $\hat{A}$  and  $\hat{B}$  for

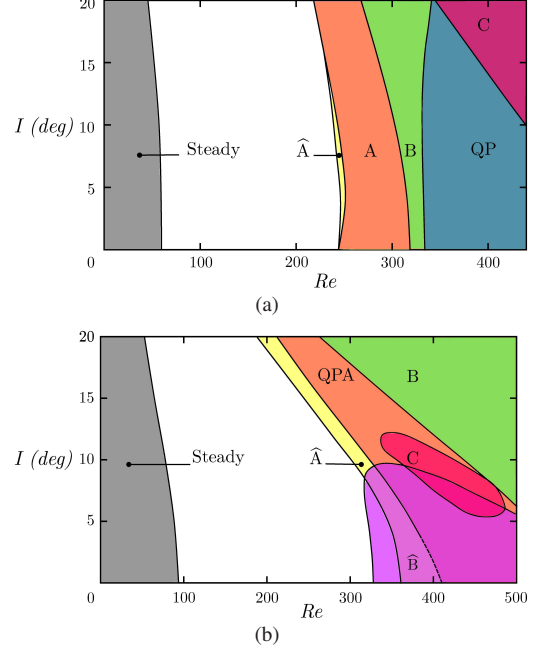


Figure 1: Marginal stability diagram of the  $Re - I$  parameter space showing the various transitions for  $Re \leq 500, I \leq 20^\circ$  for the elliptical cylinder of (a)  $AR = 1.5$  and (b)  $AR = 2.5$ . The three-dimensional modes are each assigned a unique colour and the steady region is shaded in grey.

$AR \geq 1.2$  and  $AR \geq 1.75$ . For  $AR = 1.5$ , the onset of mode  $\hat{A}$  was observed at Reynolds numbers close to the onset of mode A instability as shown in figure 1(a). As the incident angle was increased, the onset of modes A,  $\hat{A}$  and B decrease to lower Reynolds numbers, while that of mode QP increases to higher Reynolds numbers. Furthermore, at higher incident angles a subharmonic mode, mode C, is observed. The onset of mode C occurs at lower Reynolds numbers as the incident angle is increased. The boundaries of modes A and  $\hat{A}$  are contiguous for this aspect ratio and the two modes coalesce at higher Reynolds numbers [2, 20].

The parameter map for  $AR = 2.5$ , is shown in figure 1(b). The  $Re_c$  of modes  $\hat{A}$  and B decreases with incident angle and mode C forms a closed region in the parameter space. Mode  $\hat{B}$  is unstable over a large region of the parameter space and is unstable for  $I \lesssim 10^\circ$ . Of significance in this parameter space is the behaviour of mode QPA, which becomes unstable to perturbations beyond the onset of mode  $\hat{A}$ . While this mode is observed as a synchronous/real mode at low incident angles, the Floquet multipliers of this mode gradually become quasi-periodic as the incident angle is increased. The spanwise wavelength of this mode is similar to the wavelength of mode A instability and shares the same spatio-temporal characteristics of mode A at low incident angles. Hence, this mode has been labelled as mode QPA.

Shown in figure 2 is the locus of normalised Floquet multipliers on the complex plane at the specified parametric values as the incident angle is decreased. The multipliers lie on the unit circle ( $|\mu| = 1$ ) and the imaginary component of the multipliers decreases as the incident angle is decreased. For clarity, only the positive component of the complex-

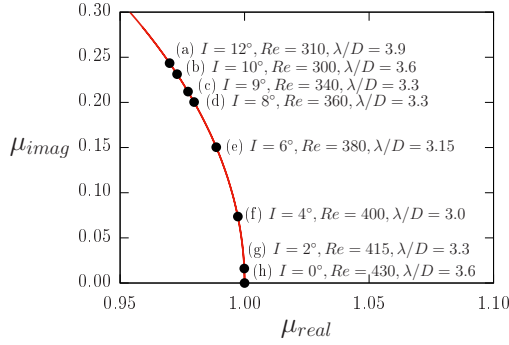


Figure 2: Locus of the normalised Floquet multipliers on the complex plane at the specified values for  $AR = 2.5$ . The values chosen are close to the marginal stability curve for mode QPA.

conjugate pair of the multipliers is shown in this figure (and also in figure 3(a)). The unit circle ( $|\mu| = 1$ ) is shown by the curved red line in these figures.

Furthermore, at a given incident angle, the Floquet multipliers of mode QPA decrease and approach the real axis as the Reynolds number is increased. Shown in figure 3 are the locus of the Floquet multipliers on the complex plane as the Reynolds number is increased for  $AR = 2.5, I = 8^\circ$ . Around  $Re = 360$ , mode QPA becomes unstable to perturbations and on further increasing the Reynolds number, the magnitude of the imaginary component of the Floquet multiplier decreases and becomes a real mode for  $Re \gtrsim 460$ . The onset of the real mode is also dependent on the spanwise wavelength. The spanwise frequency ( $St_{3D}$ ) of this mode can be computed from the Floquet multiplier by  $St_{3D} = \tan^{-1}(\mu_{imag}/\mu_{real})/(2\pi T_{2D})$ , where  $T_{2D}$  is the time period of shedding of the two-dimensional base flow. Evaluating  $St_{3D}$  at  $Re = 400$  for the above case, we obtain  $St_{3D} \simeq 0.0063187$ , which corresponds to  $\simeq 158.26$  non-dimensional time units or approximately thirty-four periods of shedding ( $T_{2D} = 4.689$ ). Shown in figures 3(b) and 3(c) are the three-dimensional reconstructions of two spanwise wavelengths of this mode using isosurfaces of streamwise vorticity (in red and yellow) at two instances that are seventeen periods apart for the cylinder (in blue) which spans  $8D$ . Clearly, the mode has traversed half a wavelength in the spanwise direction, with the isosurfaces having swapped signs. Independent three-dimensional DNS have also confirmed this behaviour (not shown here).

### Conclusions

The three-dimensional transitions in the wake of elongated bluff bodies are investigated for  $AR \leq 2.5, Re \leq 500$  and  $I \leq 20^\circ$ . Parameter maps showing the occurrence of the three-dimensional modes are presented for  $AR = 1.5$  and  $2.5$ . While modes A,  $\hat{A}$ , B and QP are observed for all incident angles; modes  $\hat{B}$  and C occur over a limited range in the  $Re - I$  parameter space investigated here. Together with the well known modes of A,  $\hat{A}$ , B,  $\hat{B}$ , C and QP, a new mode, mode QPA, having spatio-temporal characteristics and spanwise wavelength similar to that of mode A is observed. For  $AR \gtrsim 1.8$ , the imaginary component of the Floquet multiplier of mode QPA decreases as the incident angle is decreased and becomes a real mode at  $I = 0^\circ$ . For

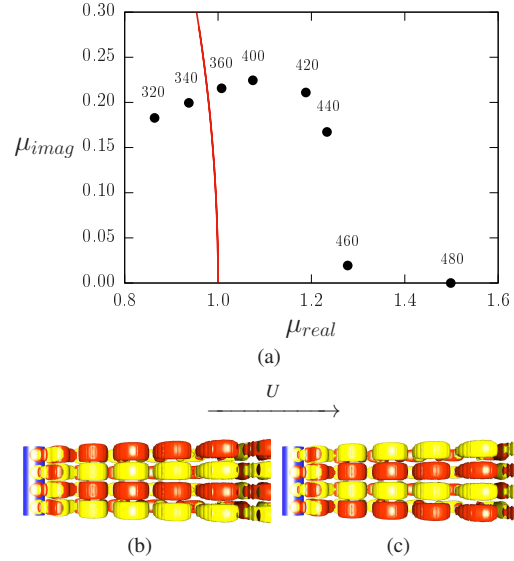


Figure 3:  $AR = 2.5, I = 8^\circ$  - (a) locus of the Floquet multipliers on the complex plane at the specified Reynolds numbers for a fixed spanwise wavelength of  $\lambda/D = 3.6$ . Three-dimensional reconstructions of mode QPA in plan view taken at (b)  $T = T_0$  and (c)  $T = T_0 + 17T$  at  $Re = 400$  showing two spanwise wavelengths of the instability.

a given incident angle, this mode is transformed to a real mode with increase in Reynolds number at a given spanwise wavelength. Thus, the wake of an elongated elliptical bluff body at incidence provides rich fluid dynamics with a variety of three-dimensional transitions occurring over a limited parameter space.

### Acknowledgements

The support from Australian Research Council Discovery Grants DP130100822, DP150102879, DP150103177 and computing time from NCI, VLSCI, NeCTAR and Monash e-Research Centre are gratefully acknowledged. The authors would also like to acknowledge the storage space provided via VicNode/RDSI grant allocation 2014R8.2.

### References

- [1] Barkley, D. and Henderson, R. D., Three-dimensional Floquet stability analysis of the wake of a circular cylinder, *Journal of Fluid Mechanics*, **322**, 1996, 215–241.
- [2] Blackburn, H. M. and Lopez, J. M., On three-dimensional quasiperiodic Floquet instabilities of two-dimensional bluff body wakes, *Physics of Fluids*, **15**, 2003, L57–L60.
- [3] Blackburn, H. M., Marques, F. and Lopez, J. M., Symmetry breaking of two-dimensional time-periodic wakes, *Journal of Fluid Mechanics*, **552**, 2005, 395–411.
- [4] Jackson, C. P., A finite-element study of the onset of vortex shedding in flow past variously shaped bodies, *Journal of Fluid Mechanics*, **182**, 1987, 23–45.

- [5] Karniadakis, G. E. and Sherwin, S. J., *Spectral/hp Methods for Computational Fluid Dynamics*, Oxford University Press, Oxford, 2005.
- [6] Kim, M.-S. and Sengupta, A., Unsteady viscous flow over elliptic cylinders at various thickness with different Reynolds numbers, *Journal of Mechanical Science and Technology*, **19**, 2005, 877–886.
- [7] Leontini, J. S., Lo Jacono, D. and Thompson, M. C., Stability analysis of the elliptic cylinder wake, *Journal of Fluid Mechanics*, **763**, 2015, 302–321.
- [8] Marques, F., Lopez, J. and Blackburn, H., Bifurcations in systems with  $Z_2$  spatio-temporal and  $O(2)$  spatial symmetry, *Physica D: Nonlinear Phenomena*, **189**, 2004, 247 – 276.
- [9] Mittal, R. and Balachandar, S., Direct numerical simulation of flow past elliptic cylinders, *Journal of Computational Physics*, **124**, 1996, 351 – 367.
- [10] Nair, M. and Sengupta, T., Unsteady flow past elliptical cylinders, *Journal of Fluids and Structures*, **11**, 1997, 555 – 595.
- [11] Paul, I., Prakash, K. A. and Vengadesan, S., Onset of laminar separation and vortex shedding in flow past unconfined elliptic cylinders, *Physics of Fluids*, **26**, 2014, 023601–1 – 023601–15.
- [12] Persillion, H. and Braza, M., Physical analysis of the transition to turbulence in the wake of a circular cylinder by three-dimensional Navier-Stokes simulation, *Journal of Fluid Mechanics*, **365**, 1998, 23–88.
- [13] Radi, A., Thompson, M. C., Rao, A., Hourigan, K. and Sheridan, J., Experimental evidence of new three-dimensional modes in the wake of a rotating cylinder, *Journal of Fluid Mechanics*, **734**, 2013, 567–594.
- [14] Rao, A., Leontini, J., Thompson, M. C. and Hourigan, K., Three-dimensionality in the wake of a rotating cylinder in a uniform flow, *Journal of Fluid Mechanics*, **717**, 2013, 1–29.
- [15] Rao, A., Leontini, J. S., Thompson, M. C. and Hourigan, K., Three-dimensionality in the wake of a rapidly rotating cylinder in uniform flow, *Journal of Fluid Mechanics*, **730**, 2013, 379–391.
- [16] Rao, A., Radi, A., Leontini, J., Thompson, M. C., Sheridan, J. and Hourigan, K., A review of rotating cylinder wake transitions, *Journal of Fluids and Structures*, **53**, 2015, 2 – 14, Special Issue on Unsteady Separation in Fluid-Structure Interaction - II.
- [17] Rao, A., Radi, A., Leontini, J. S., Thompson, M. C., Sheridan, J. and Hourigan, K., The influence of a small upstream wire on transition in a rotating cylinder wake, *Journal of Fluid Mechanics*, **769**.
- [18] Rao, A., Thompson, M. C. and Hourigan, K., A universal three-dimensional instability of the wakes of two-dimensional bluff bodies, *Journal of Fluid Mechanics*, **792**, 2016, 50–66.
- [19] Rao, A., Thompson, M. C., Leweke, T. and Hourigan, K., The flow past a circular cylinder translating at different heights above a wall, *Journal of Fluids and Structures*, **41**, 2013, 9 – 21.
- [20] Ryan, K., Thompson, M. C. and Hourigan, K., Three-dimensional transition in the wake of elongated bluff bodies, *Journal of Fluid Mechanics*, **538**, 2005, 1–29.
- [21] Sheard, G. J., Cylinders with elliptical cross-section: Wake stability with incidence angle variation, in *Proceedings of the IUTAM Symposium on Unsteady Separated Flows and Their Control*, 2007.
- [22] Sheard, G. J., Wake stability features behind a square cylinder: Focus on small incidence angles, *Journal of Fluids and Structures*, **27**, 2011, 734 – 742.
- [23] Sheard, G. J., Fitzgerald, M. J. and Ryan, K., Cylinders with square cross-section: wake instabilities with incidence angle variation, *Journal of Fluid Mechanics*, **630**, 2009, 43–69.
- [24] Sheard, G. J., Thompson, M. C. and Hourigan, K., Subharmonic mechanism of the mode C instability, *Physics of Fluids*, **17**, 2005, 1–4.
- [25] Sheard, G. J., Thompson, M. C., Hourigan, K. and Leweke, T., The evolution of a subharmonic mode in a vortex street, *Journal of Fluid Mechanics*, **534**, 2005, 23–38.
- [26] Thompson, M. C., Hourigan, K., Cheung, A. and Leweke, T., Hydrodynamics of a particle impact on a wall, *Applied Mathematical Modelling*, **30**, 2006, 1356–1369.
- [27] Thompson, M. C., Hourigan, K. and Sheridan, J., Three-dimensional instabilities in the wake of a circular cylinder, *Experimental Thermal and Fluid Science*, **12**, 1996, 190–196.
- [28] Thompson, M. C., Radi, A., Rao, A., Sheridan, J. and Hourigan, K., Low-Reynolds-number wakes of elliptical cylinders: from the circular cylinder to the normal flat plate, *Journal of Fluid Mechanics*, **751**, 2014, 570–600.
- [29] Williamson, C. H. K., The existence of two stages in the transition to three-dimensionality of a cylinder wake, *Physics of Fluids*, **31**, 1988, 3165–3168.
- [30] Williamson, C. H. K., Three-dimensional vortex dynamics in bluff body wakes, *Experimental Thermal and Fluid Science*, **12**, 1996, 150–168.
- [31] Williamson, C. H. K., Vortex dynamics in the cylinder wake, *Annual Review of Fluid Mechanics*, **28**, 1996, 477–539.
- [32] Yildirim, I., Rindt, C. C. M. and van Steenhoven, A. A., Mode C flow transition behind a circular cylinder with a near-wake wire disturbance, *Journal of Fluid Mechanics*, **727**, 2013, 30–55.
- [33] Zhang, H., Fey, U., Noack, B. R., Konig, M. and Eckelmann, H., On the transition of the cylinder wake, *Physics of Fluids*, **7**, 1995, 779–794.